Connecdenn 3/DENND1C binds actin linking Rab35 activation to the actin cytoskeleton

Andrea L. Marat, Maria S. Ioannou, and Peter S. McPherson
Department of Neurology and Neurosurgery, Montreal Neurological Institute, McGill University, Montreal, QC H3A 2B4, Canada

ABSTRACT **The small GTPase Rab35 regulates endosomal membrane trafficking but also recruits effectors that modulate actin assembly and organization. Differentially expressed in normal and neoplastic cells (DENN)–domain proteins are a newly identified class of Rab guanine-nucleotide exchange factors (GEFs) that are grouped into eight families, each activating a common Rab. The members of one family, connecdenn 1–3/DENND1A–C, are all GEFs for Rab35. Why Rab35 requires multiple GEFs is unknown. We demonstrate that connecdenn 3 uses a unique C-terminal motif, a feature not found in connecdenn 1 or 2, to directly bind actin. This interaction couples Rab35 activation to the actin cytoskeleton, resulting in dramatic changes in cell shape, notably the formation of protrusive membrane extensions. These alterations are specific to Rab35 activated by connecdenn 3 and require both the actin-binding motif and N-terminal DENN domain, which harbors the GEF activity. It was previously demonstrated that activated Rab35 recruits the actin-bundling protein fascin to actin, but the relevant GEF for this activity was unknown. We demonstrate that connecdenn 3 and Rab35 colocalize with fascin and actin filaments, suggesting that connecdenn 3 is the relevant GEF. Thus, whereas connecdenn 1 and 2 activate Rab35 for endosomal trafficking, connecdenn 3 uniquely activates Rab35 for its role in actin regulation.**

Monitoring Editor
Anne Spang
University of Basel

Received: Jun 1, 2011
Revised: Sep 23, 2011
Accepted: Nov 3, 2011

INTRODUCTION

Rabs comprise the largest family of monomeric GTPases and together with their effectors control many aspects of intracellular trafficking and organelle function, such as vesicle budding, transport, tethering, and fusion. Despite their crucial nature, for many Rabs relatively little is known about their regulation and function. Rabs need to be recruited to the correct cellular compartment, activated via guanine-nucleotide exchange factors (GEFs), which mediate the exchange of GDP to GTP, and finally turned off through the action of GTPase-activating proteins that enhance their intrinsic GTPase activity (Zerial and McBride, 2001; Stenmark, 2009; Hutagalung and Novick, 2011).

Many different enzymatic regulators of Rab GTPases contain a common, conserved protein domain. For example, TBC domain–containing proteins function broadly as GTPase-activating proteins for Rabs (Fukuda, 2011), whereas Vps9-domain proteins exhibit GEF activity with specificity for members of the Rab5 subfamily (Delprato *et al.*, 2004). Recently, proteins containing a differentially expressed in normal and neoplastic cells (DENN) domain have emerged as enzymatic regulators of Rabs (Marat and McPherson, 2010; Marat *et al.*, 2011; Allaire *et al.*, 2010; Yoshimura *et al.*, 2010). There are 18 DENN-domain proteins in humans, organized into eight families (Levivier *et al.*, 2001; Marat *et al.*, 2011), and, of interest, all proteins within a family act on a common Rab (Yoshimura *et al.*, 2010). Most of the DENN domain–containing proteins and the Rabs they target are poorly characterized.

We previously demonstrated that all three members of the connecdenn family—connecdenn 1–3 (DENND1A–C)—act as GEFs for Rab35 (Allaire *et al.*, 2010; Marat and McPherson, 2010). Rab35 has a range of cellular activities; it is found at the plasma membrane, on clathrin-coated pits and vesicles, and on endosomes (Kouranti *et al.*, 2006; Sato *et al.*, 2008; Walseng *et al.*, 2008; Chevallier *et al.*, 2009; Zhang *et al.*, 2009; Allaire *et al.*, 2010; Shim *et al.*, 2010; Uytterhoeven *et al.*, 2011). Via endosomal recruitment of EHD1, Rab35 controls a fast recycling route from early endosomes (Allaire *et al.*, 2010). A variety of cargo, including certain septins, components of the immunological synapse, MHC class I and II, exosomes,

This article was published online ahead of print in MBoC in Press (http://www.molbiolcell.org/cgi/doi/10.1091/mbc.E11-05-0474) on November 9, 2011.

Address correspondence to: Peter S. McPherson (peter.mcpherson@mcgill.ca).

Abbreviations used: AP-2, adaptor protein-2; CD, connecdenn; CST, glutathione *S*-transferase; DENN, differentially expressed in normal and neoplastic cells; GEF, guanine-nucleotide exchange factor; GTPγS, guanosine 5′-3-0-(thio) triphosphate.

and synaptic vesicle proteins, depend on Rab35 for their recycling (Heo *et al.*, 2006; Kouranti *et al.*, 2006; Patino-Lopez *et al.*, 2008; Walseng *et al.*, 2008; Allaire *et al.*, 2010; Gao *et al.*, 2010; Hsu *et al.*, 2010; Uytterhoeven *et al.*, 2011). In addition, Rab35 colocalizes with actin at the leading edge of the cell, on stress fibers, and in punctate structures within the cell (Chevallier *et al.*, 2009; Zhang *et al.*, 2009; Shim *et al.*, 2010). Expression of a constitutively active, GTP-locked form of Rab35 (Q67L) or wild-type Rab35 expressed at high levels induces morphological changes in cells, including the formation of protrusive outgrowths such as filopodia (Heo and Meyer, 2003; Patino-Lopez *et al.*, 2008; Chevallier *et al.*, 2009; Zhang *et al.*, 2009; Kanno *et al.*, 2010; Shim *et al.*, 2010). Rab35 is necessary for neurite outgrowth, and overexpression of Rab35Q67L induces the formation of unusually long extensions of the plasma membrane (Chevallier *et al.*, 2009). Rab35 also controls actin remodeling during phagocytosis, although it does not have a direct effect on actin polymerization; instead, it controls the location of polymerization (Shim *et al.*, 2010). A role for Rab35 in regulating the location of actin assembly was also seen in a study that identified fascin as a downstream Rab35 effector (Zhang *et al.*, 2009). Fascin is an actin cross-linking protein that organizes F-actin into tight, parallel bundles. Fascin binds preferentially to GTP-Rab35 and depends upon Rab35 for localization to actin at the plasma membrane, where it impacts actin structures (Zhang *et al.*, 2009).

Why do single Rabs require multiple DENN-domain GEFs? In the case of the connecdenn/DENND1 family, we now suggest that different connecdenns mediate localized Rab35 activation to control its diverse functions. Connecdenn 1, like Rab35 is required for normal endosome morphology and for endosomal recycling of MHC class I (Allaire *et al.*, 2010). Loss of connecdenn 2 also results in enlargement and perinuclear clustering of early endosomes (Marat and McPherson, 2010). Thus connecdenn 1 and 2 both appear important for activating Rab35 toward its control of endosome function. In contrast, we now demonstrate that connecdenn 3 uses a short sequence in its C-terminus, a feature not shared with the other family members, to bind directly to actin. Connecdenn 3 localizes Rab35 to actin filaments, where it exerts its role on actin dynamics. These results indicate that different DENN-domain proteins targeting the same Rab can activate that Rab toward different cellular functions.

RESULTS

Connecdenn 3 is a Rab35 GEF

We previously identified all three members of the connecdenn/DENND1 family as Rab35 GEFs, with the GEF activity mediated by the N-terminal DENN domains (Allaire *et al.*, 2010; Marat and McPherson, 2010). We thus set out to examine why Rab35 requires three separate GEFs. However, a subsequent study exploring the GEF activity of multiple DENN-domain proteins, although confirming that connecdenn 1/DENND1A and connecdenn 2/DENND1B have GEF activity toward Rab35, found that connecdenn 3/DENND1C is a GEF for Rab13 but not Rab35 (Yoshimura *et al.*, 2010). Thus it became vital for our study to examine the specificity of connecdenn 3 for Rab13 versus Rab35.

We previously demonstrated that the DENN domain of each connecdenn binds to Rab35 (Allaire *et al.*, 2010; Marat and McPherson, 2010). To test for possible binding to Rab13, we performed affinity selection studies using glutathione *S*-transferase (GST)–Rab35 and GST-Rab13, as well as GST-Rab1, in either nucleotide-free or GTPγS-loaded forms. Consistent with our previous studies, FLAG-tagged DENN domains of connecdenn 1–3 each binds Rab35 in the nucleotide-free form, a hallmark feature of GEFs, with the strongest binding for connecdenn 1 and 2 (Figure 1A; Allaire *et al.*, 2010; Marat and McPherson, 2010). We also observe slight binding between connecdenn 1 and nucleotide-free Rab1A, likely due to the sequence similarity between Rab35 and Rab1A, which are part of the same Rab subfamily. Of interest, we also see binding of connecdenn 2 and 3 DENN domains to Rab13, although the binding is slightly better in the GTPγS-loaded form (Figure 1A). Although binding of a protein to the GTP-loaded form of a Rab is generally inconsistent with GEFs, there are known exceptions (Liao *et al.*, 1999, 2001; Saito *et al.*, 2002). Therefore we examined whether the DENN domains of connecdenn 2 and 3 possess GEF activity toward Rab13.

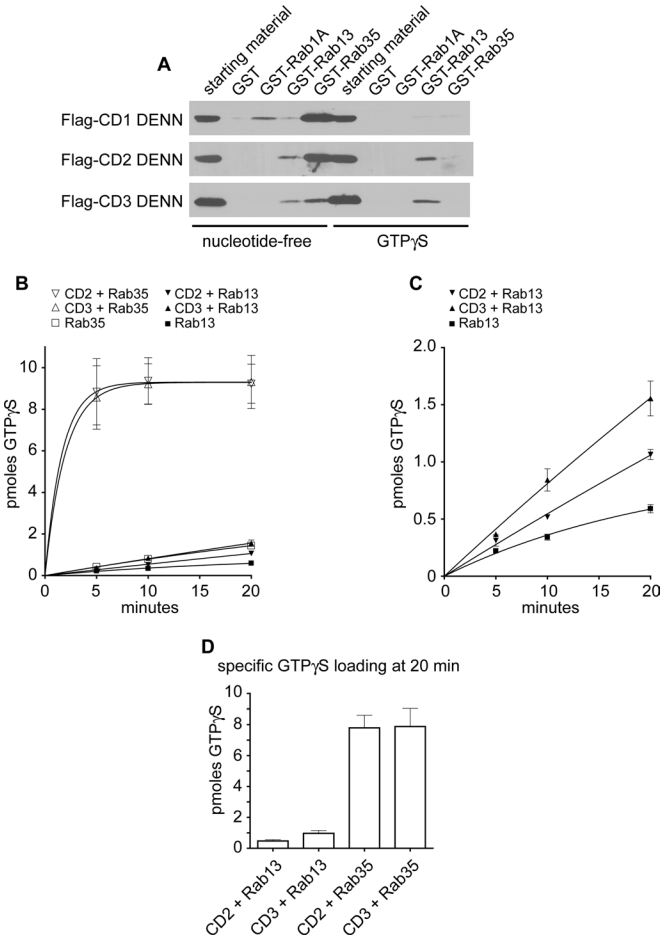

FIGURE 1: The DENN domain of connecdenn 3 exhibits higher GEF activity toward Rab35 than Rab13. (A) GST, GST-Rab1A, GST-Rab13, and GST-Rab35, maintained in the nucleotide-free state with 5 mM EDTA or preloaded with GTPγS, were used as bait in affinity selection assays with soluble lysates from HEK-293T cells transfected with FLAG-tagged DENN domains of connecdenn (CD) 1–3. Specifically bound proteins were detected by anti-FLAG antibody. Cell lysate (starting material) equivalent to 1/10 that added to the beads was analyzed in parallel. (B) GEF activity of 350 nM purified DENN domains of connecdenn 2 and 3 (CD2/CD3) or basal exchange activity of Rab13 or Rab35 alone measured as the incorporation of [^{35}S]GTPγS onto 1.25 μM GDP-loaded Rab13 or Rab35 as a function of time. The number of picomoles of incorporated GTPγS is plotted over time, and points represent mean (± SE), n = 2. (C) The exchange activity of the connecdenn 2 and 3 DENN domains against Rab13 from B plotted on an expanded scale. (D) Specific amount of GTPγS loaded onto 1.25 μM Rab13 or Rab35 in the presence of connecdenn 2 or connecdenn 3 DENN domains after 20 min was determined by subtracting the amount of GTPγS loaded in the absence of DENN domains.

Consistent with our earlier studies, purified connecdenn 2 and 3 DENN domains possess robust Rab35 GEF activity (Figure 1B; Marat and McPherson, 2010). We also see GEF activity toward Rab13 with both connecdenn 2 and 3 (Figure 1B), which is best appreciated when plotted on an expanded scaled (Figure 1C). However, GEF activity toward Rab13 is much weaker; for example, when comparing the specific GTP loading after 20 min, the GEF activity of both connecdenn 2 and 3 toward Rab35 is almost 10-fold higher than toward Rab13 (Figure 1D). Furthermore, in order to observe GEF activity toward Rab13, we need to use higher amounts of purified DENN domain than in our previous studies examining activity on Rab35, 350 nM as opposed to 100–150 nM (Allaire *et al.*, 2010; Marat and McPherson, 2010). Thus, under our experimental conditions, the DENN domain of connecdenn 3 prefers Rab35 as a substrate when compared with Rab13.

The GEF assays in Yoshimura *et al.* (2010) used full-length immunoprecipitated connecdenn 3. It is thus possible that there is additional GEF activity in connecdenn 3 toward Rab13 located in a region outside of the DENN domain. Moreover, there is the potential for autoinhibition that could explain a lack of activity of full-length connecdenn 3 toward Rab35 (Yoshimura *et al.*, 2010). For instance, through a Dbl homology domain, intersectin-long functions as a GEF for Cdc42, but the full-length form has greatly diminished activity compared with the isolated domain due to intramolecular autoinhibition (Hussain *et al.*, 2001). However, we detect no GEF activity of full-length immunoprecipitated connecdenn 3 toward Rab13 when compared with immunoprecipitations from mock-transfected cells, whereas there is GEF activity toward Rab35 (Figure 2, A and B). Taken together, our data indicate that connecdenn 3 has GEF activity for Rab13 but that it strongly prefers Rab35.

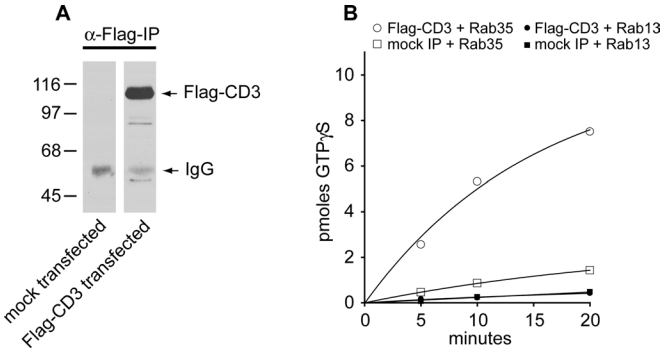

FIGURE 2: Full-length connecdenn 3 exhibits GEF activity toward Rab35 but not Rab13. (A) HEK-293T cells were transfected with full-length FLAG-tagged connecdenn 3 (CD3) or were mock transfected, and cell lysates were processed for immunoprecipitation with α-FLAG antibody, followed by detection with α-FLAG antibody. (B) Immunoprecipitated connecdenn 3 or mock immunoprecipitations were used in GEF assays measured as the incorporation of [^{35}S]GTPγS onto 1.25 μM GDP-loaded Rab13 or Rab35 as a function of time. The number of picomoles of incorporated GTPγS is plotted over time. A representative plot is shown.

Colocalization of connecdenn 3 and actin

Connecdenn 1 and 2 activate Rab35 for its role in endosomal trafficking, whereas the biological function of connecdenn 3 has not been examined (Allaire *et al.*, 2010; Marat and McPherson, 2010). To explore whether connecdenn 3 has distinct or overlapping functions with the other connecdenns, we compared the localization of FLAG-tagged proteins following their transfection in HeLa cells. Both FLAG-tagged connecdenn 1 and 2 exhibit a punctate staining pattern (Figure 3A), consistent with earlier observations that they localize in part to clathrin-coated pits (Allaire *et al.*, 2006; Marat and McPherson, 2010). In contrast, FLAG-connecdenn 3 has a partially filamentous pattern, prompting us to costain with fluorescently conjugated phalloidin, a marker of F-actin. FLAG-connecdenn 3 partially colocalizes with F-actin, especially at the edge of cells (Figure 3A). This is best appreciated in confocal Z-stacks, in which the colocalization of FLAG-connecdenn 3 with actin becomes greater as the images move from the ventral side of the cell (Figure 3B, image 1) to the cortical actin at the top of the cell (Figure 3B, images 5–8). Quantification of numerous such stacks reveals that 78.8 ± 2.6% (SEM) of FLAG-connecdenn 3 is colocalized with F-actin. Colocalization between FLAG-connecdenn 3 and F-actin is also seen in confocal stacks of COS-7 and NIH-3T3 (Supplemental Figure S1, A and B). Thus, unlike connecdenn 1 and 2, connecdenn 3 appears to be associated with F-actin.

Connecdenn 3 contains a C-terminal actin-localization signal

We next explored the mechanism by which connecdenn 3 localizes to actin. The isolated DENN domain of connecdenn 3 gives a soluble staining pattern when expressed in cells (Supplemental Figure S2), suggesting that the actin-localization signal is located outside the DENN domain. Examination of the C-terminal region reveals surprisingly limited evolutionary conservation, even when comparing human to mouse (Figure 4A). However, there is a well-conserved block covering the last 12 amino acids (Figure 4A), and this segment is conserved throughout evolution (Figure 4B). The sequence is not present in connecdenn 1 or 2. To determine whether this sequence is involved in targeting connecdenn 3 to actin, we deleted the last 16 amino acids (CD3 Δ786–801). This deletion abolishes the actin colocalization seen with full-length connecdenn 3 (Figure 4C). Treatment of cells with latrunculin B, an actin-depolymerizing drug, causes actin to appear in large, clustered punctae, and connecdenn 3 relocalizes to these punctae (Figure 4D). Connecdenn 3 Δ786–801 fails to redistribute to actin aggregates after latrunculin B treatment (Figure 4D). Thus the conserved C-terminal segment of connecdenn 3 mediates actin colocalization.

Connecdenn 3 contains a C-terminal actin-binding sequence

We next sought to examine whether connecdenn 3 binds to actin. Soluble HeLa cell lysates expressing FLAG-tagged connecdenn proteins were incubated in the absence or presence of highly purified nonmuscle actin that had been prepolymerized into F-actin. Following incubation, the samples were subjected to high-speed centrifugation, and the supernatant (S) and F-actin–rich pellets (P) were examined by Western blot. A significant component of full-length connecdenn 3 appears in the pellet fraction only in the presence of F-actin, whereas very little connecdenn 3 Δ786–801 is seen in the pellet (Figure 5A). There is no specific sedimentation of either connecdenn 1 or 2 (Figure 5A). Thus connecdenn 3 specifically cosediments with F-actin, and the interaction depends on amino acids within the region from 786 to 801. To determine whether the C-terminal segment is sufficient for actin binding and to better define the binding site, we generated a GST fusion protein encoding residues 789–801. This fusion protein binds to actin from rat brain homogenates, with no binding to other abundant proteins, such as tubulin and the clathrin adaptor AP-2 (Figure 5B). A series of double point mutations of six highly conserved residues within the binding site (DL-794-AA, KK-796-AA, FE-799-AA; Figure 4B) abolishes actin binding (Figure 5B). Thus connecdenn 3 binds specifically to actin, and the C-terminal segment is critical for this interaction.

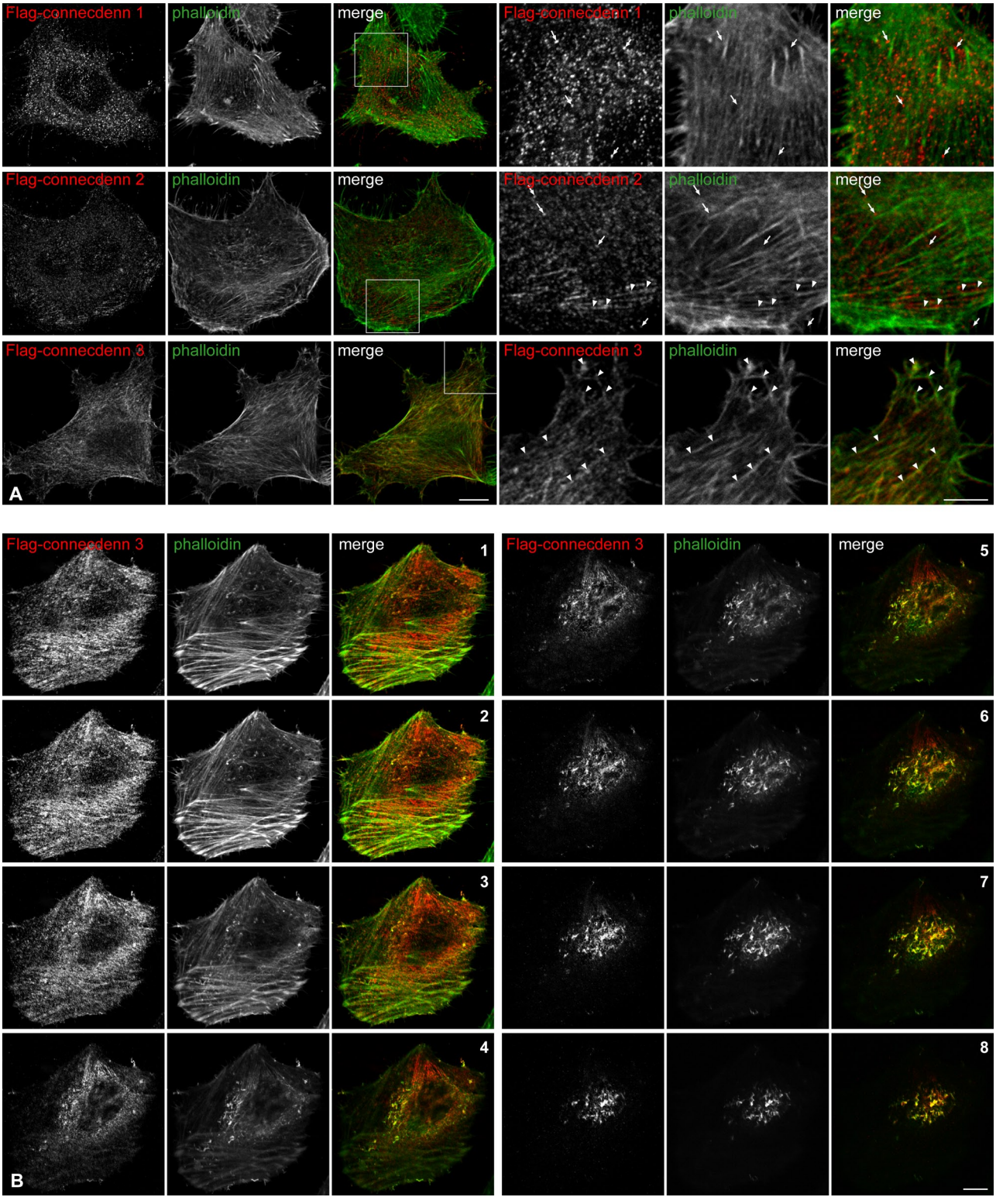

FIGURE 3: Connecdenn 3 colocalizes with actin. (A) HeLa cells were transfected with FLAG-tagged full-length connecdenn 1, connecdenn 2, or connecdenn 3 as indicated and processed for immunofluorescence with a monoclonal antibody against the FLAG tag (red) after short transfection times to minimize overexpression. Actin was visualized by costaining with fluorescein isothiocyanate (FITC)–labeled phalloidin (green). Nine rightmost, magnified views from the regions indicated by boxes. Connecdenn 1 punctae (arrows) do not colocalize with actin filaments. Connecdenn 2 punctae (arrows) do not colocalize with actin, although some are found adjacent to actin filaments (arrowheads). Connecdenn 3 colocalizes with actin filaments (arrowheads). Scale bars, lower magnification, 10 μm; higher magnification, 5 μm. (B) HeLa cells were transfected and processed for immunofluorescence as in A. Z-stacks were taken every 0.36 μm from the ventral side (1) to the dorsal side (8). Scale bars, 10 μm.

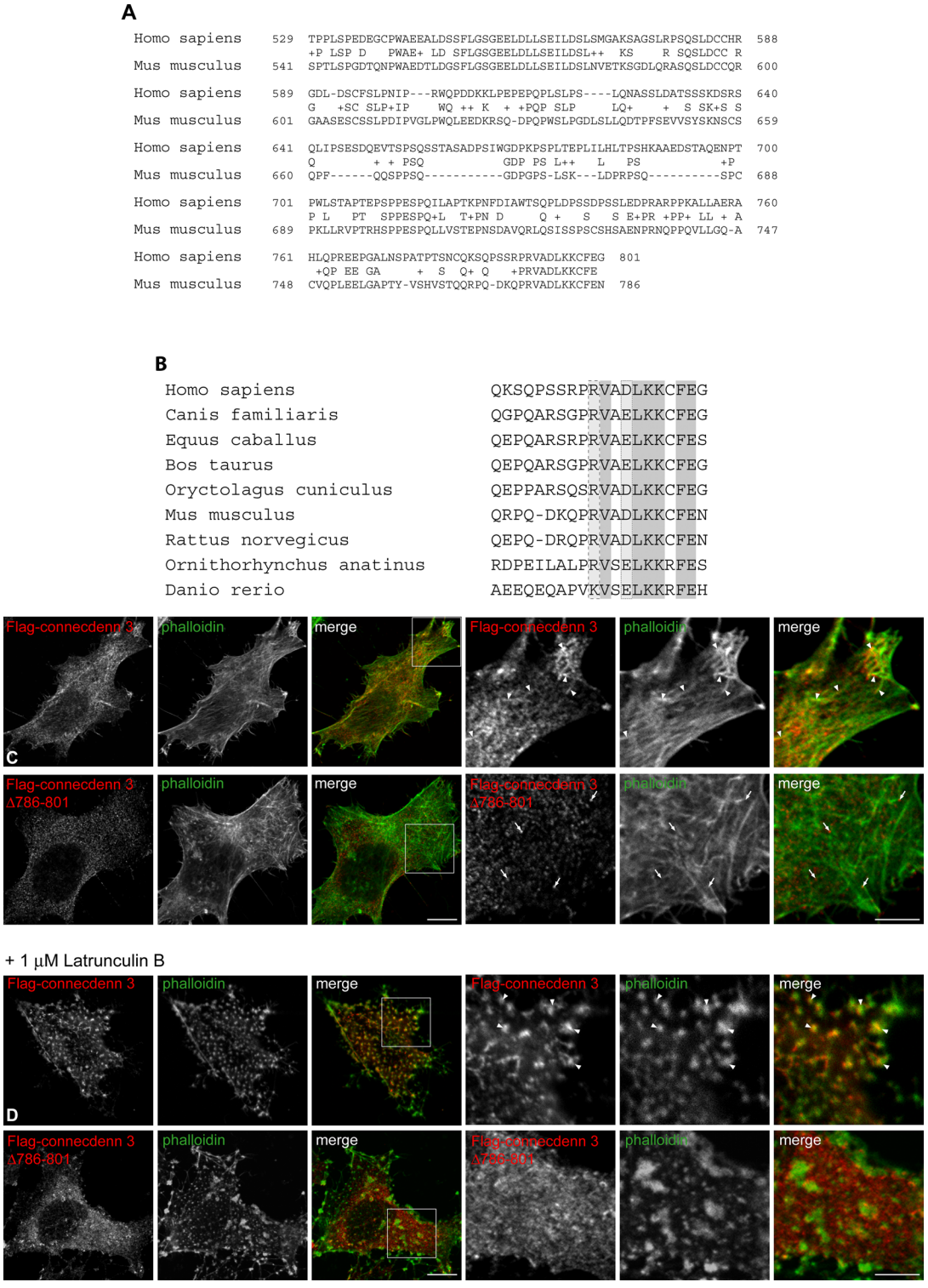

FIGURE 4: Colocalization of connecdenn 3 with actin is mediated by a conserved C-terminal motif. (A) Alignment of the C-terminal regions of human (gi74750652) and mouse (gi24025656) connecdenn 3. Identical amino acids are written, and conserved residues are indicated by a plus sign. (B) Alignment of the 20 C-terminal residues of connecdenn 3 throughout species. Identical amino acids are shaded dark gray, and conserved acidic and basic residues are indicated by light gray boxes with dotted and dashed outlines, respectively. (C) HeLa cells were transfected with FLAG-tagged full-length connecdenn 3 or connecdenn 3 with a deletion of the last 16 residues (Δ786–801) and processed for immunofluorescence with a monoclonal antibody against the FLAG tag (red) after short transfection times to minimize overexpression. Actin was visualized by costaining with FITC-labeled phalloidin (green). A merged image is indicated. Six rightmost, magnified views from the regions indicated by boxes. (D) As for C except that prior to fixation, cells were treated with 1 μM latrunculin B for 10 min at 37°C. For C and D, arrowheads indicate areas of colocalization of connecdenn 3 and actin filaments (C) or focal actin aggregates (D), whereas connecdenn 3 Δ786–801 does not colocalize with actin (arrows). Scale bars, lower magnification, 10 μm; higher magnification, 5 μm.

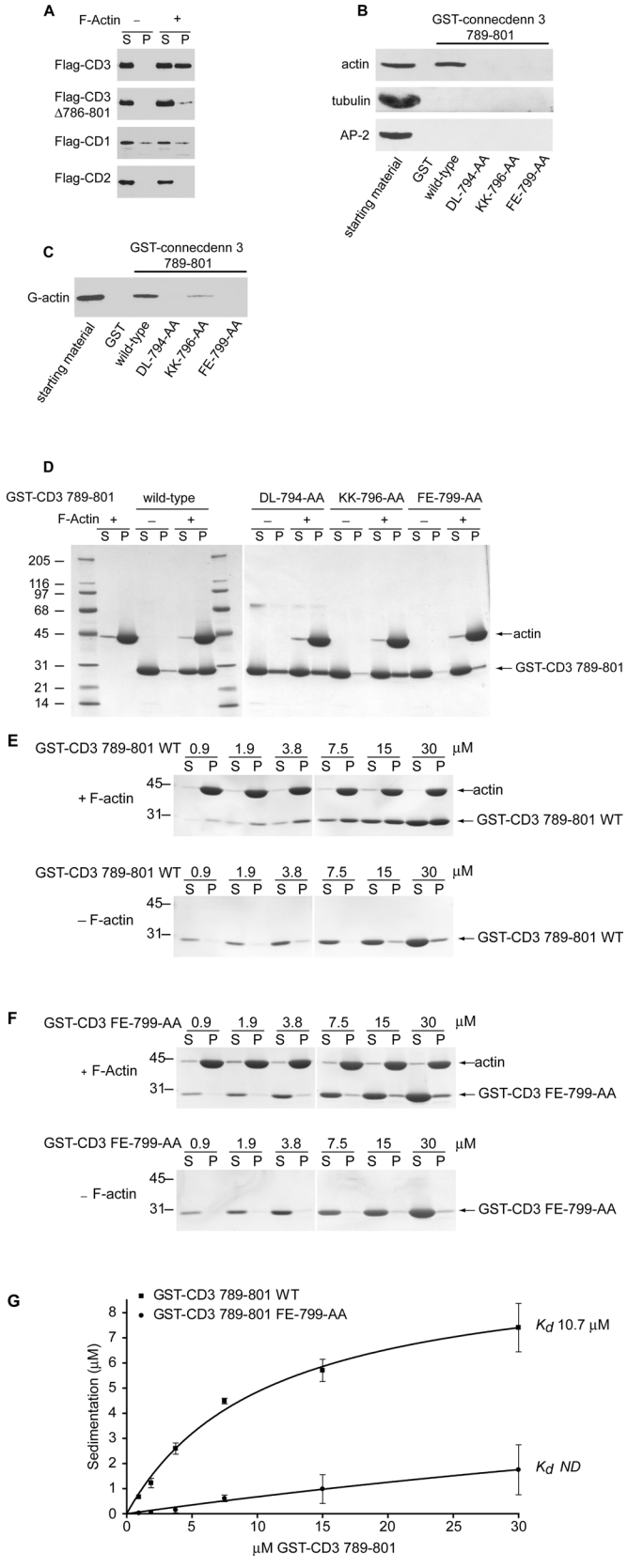

FIGURE 5: Connecdenn 3 binds directly to both G- and F-actin through its C-terminal motif. (A) Soluble lysates of HEK-293T cells transfected with FLAG-connecdenn 1 (CD1), connecdenn 2 (CD2), or connecdenn 3 (CD3) or full-length or CD3 Δ786–801 were incubated in the absence (–) or presence (+) of 18 μM polymerized nonmuscle actin and then centrifuged at high speed. The supernatant (S) and pellet (P) fractions were analyzed by Western blotting against the FLAG epitope. (B) Soluble rat brain extract was incubated with GST or equimolar amounts of wild-type GST fusion protein encoding amino acids 789–801 of connecdenn 3 or the same construct containing the indicated double point mutations, precoupled to glutathione–Sepharose. An aliquot of the lysate (starting material) equivalent to 1/10 that added to the beads was analyzed in parallel. Western blotting against endogenous actin, tubulin, or α-adaptin (AP-2) revealed specifically bound protein. (C) Aliquots of 50 nM of nonmuscle G-actin were incubated with GST or equimolar amounts of wild-type GST fusion protein encoding amino acids 789–801 of connecdenn 3 or the same construct containing the indicated double point mutations, precoupled to glutathione–Sepharose. An aliquot of the lysate (starting material) equivalent to 1/10 that added to the beads was analyzed in parallel. Western blotting against actin revealed specifically bound protein. (D) Purified GST-connecdenn 3 789–801 in the wild-type form or with the indicated double point mutations (15 μM) was incubated in the absence (–) or presence (+) of 18 μM polymerized nonmuscle actin and then centrifuged at high speed. The supernatant (S) and pellet (P) fractions were resolved by SDS–PAGE and stained with Coomassie blue to reveal pelleted F-actin and the degree of free and bound GST-connecdenn 3. (E, F) The indicated molar amounts of GST-connecdenn 3 789–801 wild type (WT) (E) or FE-799-AA double mutation (F) were incubated in the absence (–) or presence (+) of 18 μM polymerized nonmuscle actin and then centrifuged at high speed. The supernatant (S) and pellet (P) fractions were resolved by SDS–PAGE and stained with Coomassie blue to reveal pelleted F-actin and the degree of free and bound GST-connecdenn 3. (G) Quantification of GST-connecdenn 3 789–801 wild type (WT) and FE-799-AA double mutant specifically cosedimenting with F-actin reveals dissociation constants of ~10.7 μM and not determinable (ND).

To examine whether actin binding is direct, and to assess whether connecdenn 3 binds G-actin, F-actin, or both, we performed additional binding studies using purified nonmuscle actin. An affinity selection assay using GST-connecdenn 3 789–801 reveals direct binding to purified G-actin (Figure 5C). Double mutations DL-794-AA and FE-799-AA abolish binding, whereas the KK-796-AA mutation reduces binding (Figure 5C). We then performed F-actin cosedimentation experiments in which purified GST-connecdenn 3 789–801, wild-type, and mutants were incubated in the absence or presence of purified, preassembled F-actin. Following incubation, the samples were subjected to a high-speed centrifugation, and the supernatant (S) and F-actin–rich pellets (P) were examined by Coomassie staining (Figure 5D). Whereas wild-type GST fusion protein sediments specifically in the presence of F-actin, the mutants DL-794-AA and FE-799-AA have essentially no F-actin binding, and KK-796-AA has reduced binding (Figure 5D). Thus connecdenn 3 binds specifically to both G- and F-actin using selected residues in the C-terminal binding site.

To determine the approximate affinity of the interaction, we performed F-actin sedimentation assays with increasing concentrations of GST-CD3 789–801 or the FE-799-AA double mutant (Figure 5, E and F). The Coomassie-stained gels were scanned to quantify the amount of peptide specifically sedimenting in the F-actin–rich pellets, revealing that the wild-type actin-binding sequence has a dissociation constant of ~10.7 μM (Figure 5G). This affinity is similar to that of other actin-binding proteins, such as ADF/cofilin, Arp2/3, and thymosin β4 (Van *et al.*, 1996; dos Remedios *et al.*, 2003). In contrast, the binding affinity of the FE-799-AA double mutant was too low to be measured (Figure 5G). Together, these data demonstrate that connecdenn 3 exhibits direct binding to actin. When considering the results of the mutational studies in the context of the

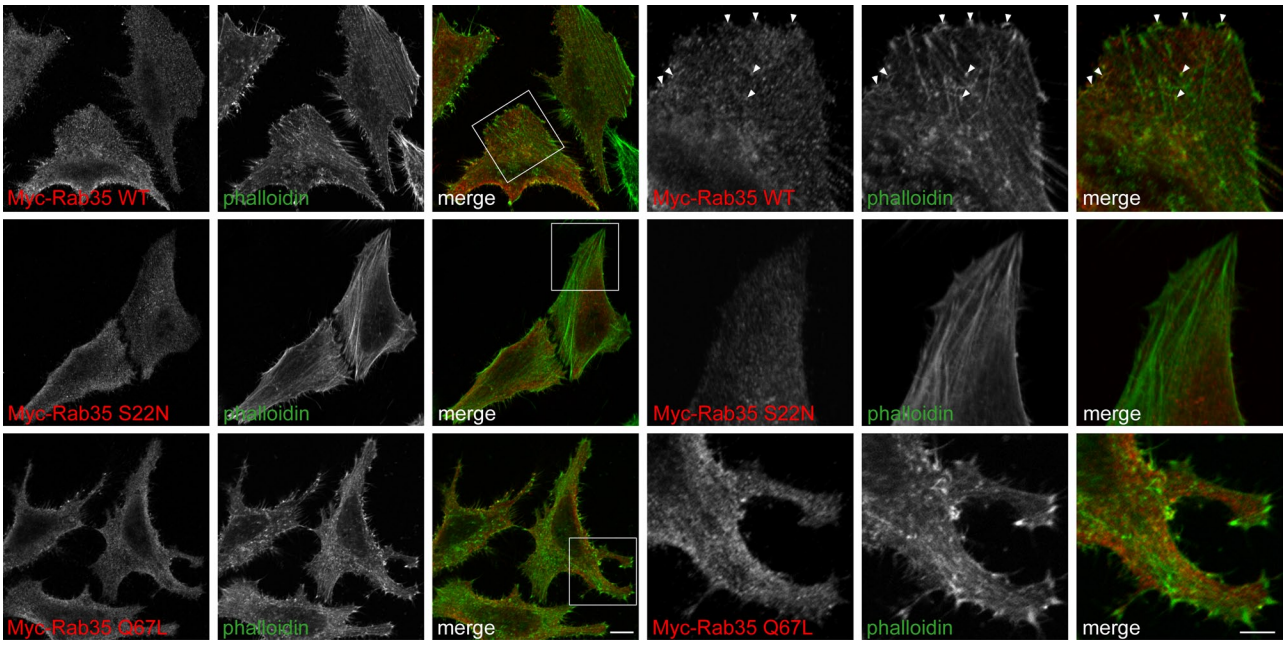

FIGURE 6: Effect of Rab35 on HeLa cell morphology. HeLa cells were transfected with Myc-tagged wild-type (WT) Rab35, dominant-negative Rab35 S22N, or constitutively active Rab35 Q67L and processed for immunofluorescence with a polyclonal antibody against the Myc tag (red). Actin was visualized by costaining with FITC labeled phalloidin (green). Nine rightmost, magnified views from the regions indicated by boxes. Arrowheads indicate colocalization between wild-type Rab35 and actin filaments. Scale bars, lower magnification, 10 μm; higher magnification, 5 μm.

evolutionary conservation of the C-terminal region (Figure 4B), we suggest a sequence of [R/K]V[A/S][D/E]LKKxFE as responsible for actin binding in connecdenn 3.

Active Rab35 causes changes in cell morphology

Previous studies showed that Rab35 colocalizes in part with actin and that alterations in Rab35 activity influence cell morphology. For example, expression of constitutively active Rab35 in BHK cells leads to unusually long cell extensions (Chevallier *et al.*, 2009). In fact the production of protrusive outgrowths is characteristic of Rab35 activation in multiple cell types, including *Drosophila* S2 and SL2 cells, NIH-3T3 cells, and Jurkat T cells (Heo and Meyer, 2003; Patino-Lopez *et al.*, 2008; Zhang *et al.*, 2009; Chua *et al.*, 2010; Shim *et al.*, 2010). We therefore examined the effect of expressing low levels of Myc-tagged Rab35 in HeLa cells. Consistent with what others reported (Chevallier *et al.*, 2009; Zhang *et al.*, 2009; Shim *et al.*, 2010), we observe a small degree of colocalization between actin and either wild-type Rab35 or constitutively active, GTP-locked Rab35 Q67L, which was not observed with the dominant-negative, GDP-locked mutant Rab35 S22N (Figure 6). Furthermore, constitutively active Rab35 Q67L expressed at relatively low levels has an effect on HeLa cell morphology, resulting in protrusive outgrowths, including filopodia (Figure 6). Therefore, similar to what occurs in other cell types (Heo and Meyer, 2003; Patino-Lopez *et al.*, 2008; Chevallier *et al.*, 2009; Zhang *et al.*, 2009; Kanno *et al.*, 2010; Shim *et al.*, 2010), Rab35 colocalizes with actin, and active Rab35 causes changes in cell morphology in HeLa cells.

Connecdenn 3 specifically targets Rab35 to actin

Although the influence of activated Rab35 on actin dynamics and cell morphology is well established, the relevant GEF to activate Rab35 for these effects is unknown (Zhang *et al.*, 2009). Given our results, it seems likely that connecdenn 3 could serve this role. We thus coexpressed connecdenn 3 with wild-type Rab35, resulting in dramatic changes in cell morphology, notably the formation of long cellular extensions and protrusions, including filopodia (Figure 7A). The effect on cell morphology of connecdenn 3 coexpressed with wild-type Rab35 is even more obvious than that of Rab35 Q67L (Figure 6). We also observe colocalization of connecdenn 3, Rab35 and actin (Figure 7A), whereas wild-type myc-Rab35 expressed at low levels has minimal colocalization with actin on its own (Figure 6). Coexpression of wild-type Rab35 with connecdenn 1 or with connecdenn 3 Δ786–801 does not result in changes in cell morphology or an increase in Rab35 colocalization with actin (Figure 7, B and C). Finally, we coexpressed wild-type Rab35 with a connecdenn 3 construct that lacks the DENN domain (Δ1–424) and therefore cannot activate Rab35. The colocalization of connecdenn 3 Δ1–424 with actin is maintained (Supplemental Figure S3); however, we do not observe changes in cell morphology or increased Rab35 colocalization with actin (Supplemental Figure S4). Thus it appears that connecdenn 3 is the GEF that activates Rab35 for its effects on actin dynamics and cell morphology, using the combination of a C-terminal actin-binding motif and an N-terminal DENN domain.

Connecdenn 3 is required for the proper targeting of Rab35 to actin

Previous studies examining the role of Rab35 on actin dynamics showed that Rab35 knockdown inhibits neurite outgrowth, results in abnormal bristle morphology in *Drosophila*, and inhibits the formation of membrane ruffles (Chevallier *et al.*, 2009; Zhang *et al.*, 2009; Shim *et al.*, 2010). We attempted to investigate the effects of connecdenn 3 knockdown on Rab35-mediated actin dynamics but were unable to obtain a reproducible knockdown despite using multiple connecdenn 3–specific siRNA sequences in different cell lines (data not shown). We therefore used the DENN domain of connecdenn 3 as a dominant-negative construct. GEFs likely have a crucial role in Rab targeting; for example, the DrrA GEF from *Legionella pneumophila* displaces Rab1 from the Rab1:GDI complex, resulting in the

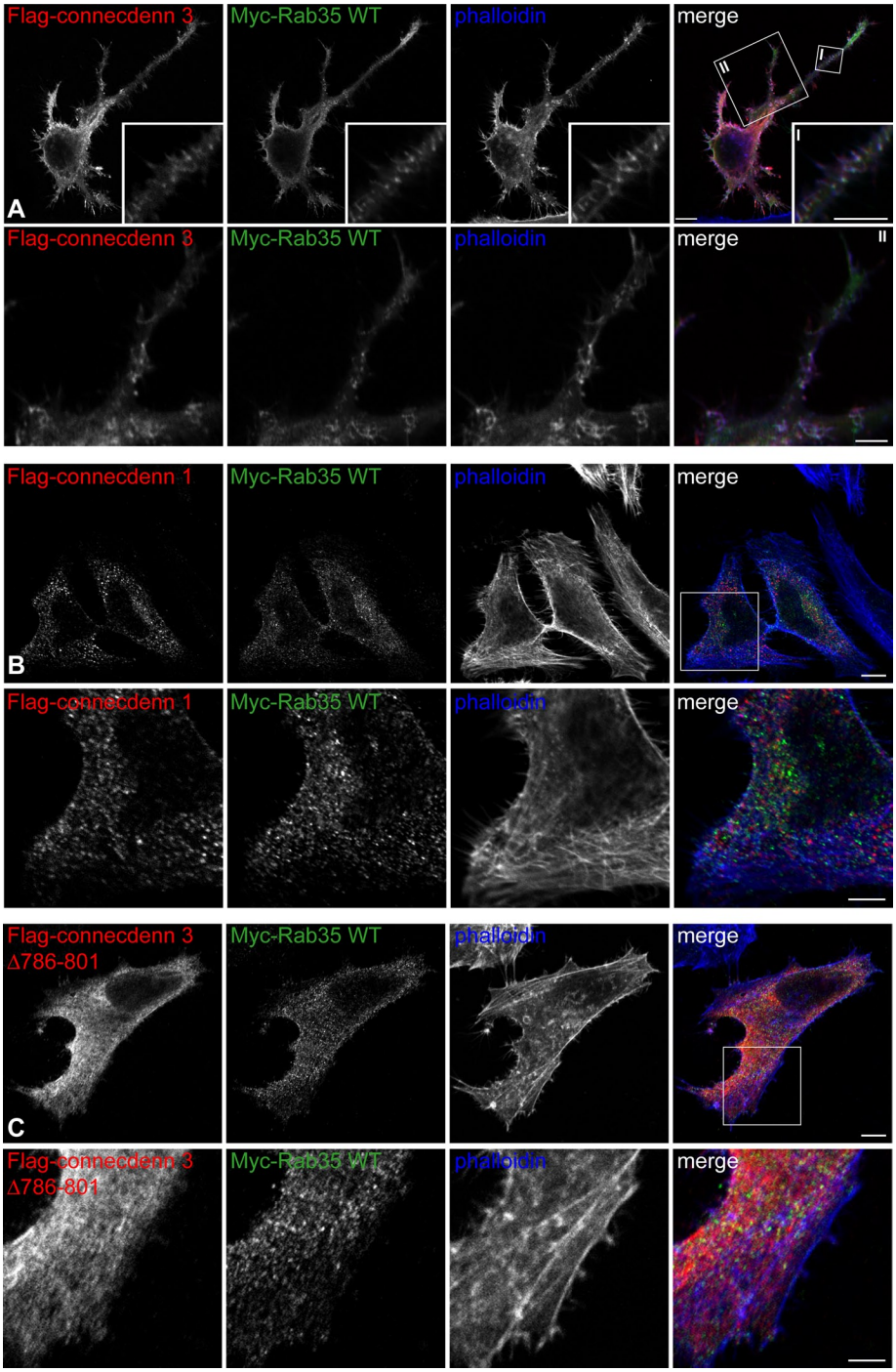

FIGURE 7: Connecdenn 3 targets Rab35 to actin filaments, resulting in morphological changes. (A) HeLa cells were cotransfected with FLAG-tagged connecdenn 3 and Myc-tagged wild-type Rab35 and processed for immunofluorescence with a monoclonal antibody against the FLAG tag (red) and a polyclonal antibody against the Myc tag (green). Actin was visualized by costaining with Alexa Fluor 647–labeled phalloidin (blue). The boxed area indicated by I is shown in the inset, and the boxed area indicated by II is shown below. Scale bars, lower magnification, 10 μm; higher magnification I and II, 2.5 and 5 μm, respectively. (B) As for A, except that cells were transfected with connecdenn 1 instead of connecdenn 3. (C) As for A, except that cells were transfected with connecdenn 3 lacking the last 16 amino acids, Δ786–801. Scale bars, B and C, lower magnification, 10 μm; higher magnification, 5 μm.

mistargeting of Rab1 to the membrane of the *Legionella*-containing vacuole (Schoebel *et al.*, 2009). We therefore hypothesized that overexpressing FLAG-connecdenn 3 DENN domain, which cannot bind actin, would result in the mistargeting of Rab35, thereby ablating its effects on actin dynamics. Similar to what was reported by others using high overexpression levels of wild-type Rab35 (Patino-Lopez *et al.*, 2008; Chevallier *et al.*, 2009; Zhang *et al.*, 2009; Kanno *et al.*, 2010; Shim *et al.*, 2010), we found overexpression of higher levels of green fluorescent protein (GFP)–Rab35 wild type on its own, compared with the lower levels of myc-Rab35 used previously, results in protrusive outgrowths, and colocalization is seen between GFP-Rab35 and actin (Figure 8A). When GFP-Rab35 wild type was coexpressed with the FLAG-tagged connecdenn 3 DENN domain, we observed that GFP-Rab35 was no longer colocalized with actin at the cell periphery and that the morphological changes induced by Rab35 overexpression were ablated (Figure 8B).

Relationship between connecdenn 3, Rab35, and fascin

Fascin is an actin–cross-linking protein that organizes F-actin into parallel bundles in protruding structures at the leading edge of cells (Adams *et al.*, 1999; Vignjevic *et al.*, 2006). Scott and colleagues demonstrated that Rab35 binds fascin preferentially in a GTP bound form and that Rab35 and fascin colocalize (Zhang *et al.*, 2009). Although Rab35 does not bind actin or have an effect on actin bundling itself, it controls the recruitment of fascin, which then bundles actin. This leads to striking morphological changes—notably alterations in general cell shape, the presence of large protrusive outgrowths, and increased filopodia (Zhang *et al.*, 2009). The relevant GEF for activating Rab35 in this pathway is unknown. However, since connecdenn 3 targets Rab35 to actin filaments resulting in morphological changes similar to those seen in other studies (Zhang *et al.*, 2009; compare Supplemental Figure S10 of that study to Figure 7A), we hypothesized that connecdenn 3 would be the GEF responsible for fascin recruitment. Similar to what was reported (Zhang *et al.*, 2009), we observe a degree of colocalization between Rab35 and fascin near the plasma membrane (Figure 9A), and this is enhanced when we coexpress connecdenn 3 (Figure 9B). Consistent with the triple colocalization observed between connecdenn 3, Rab35, and actin filaments, connecdenn 3, Rab35, and fascin colocalize (Figure 9B). Together, these data support a model in which Rab35 mediates the formation of cellular protrusions (Figure 9C). Connecdenn 3 is recruited to actin via its C-terminal actin-binding motif; it then mediates the GDP-to-GTP exchange on Rab35 via its DENN domain. GTP-Rab35 recruits its effector, fascin, resulting in the bundling of actin filaments.

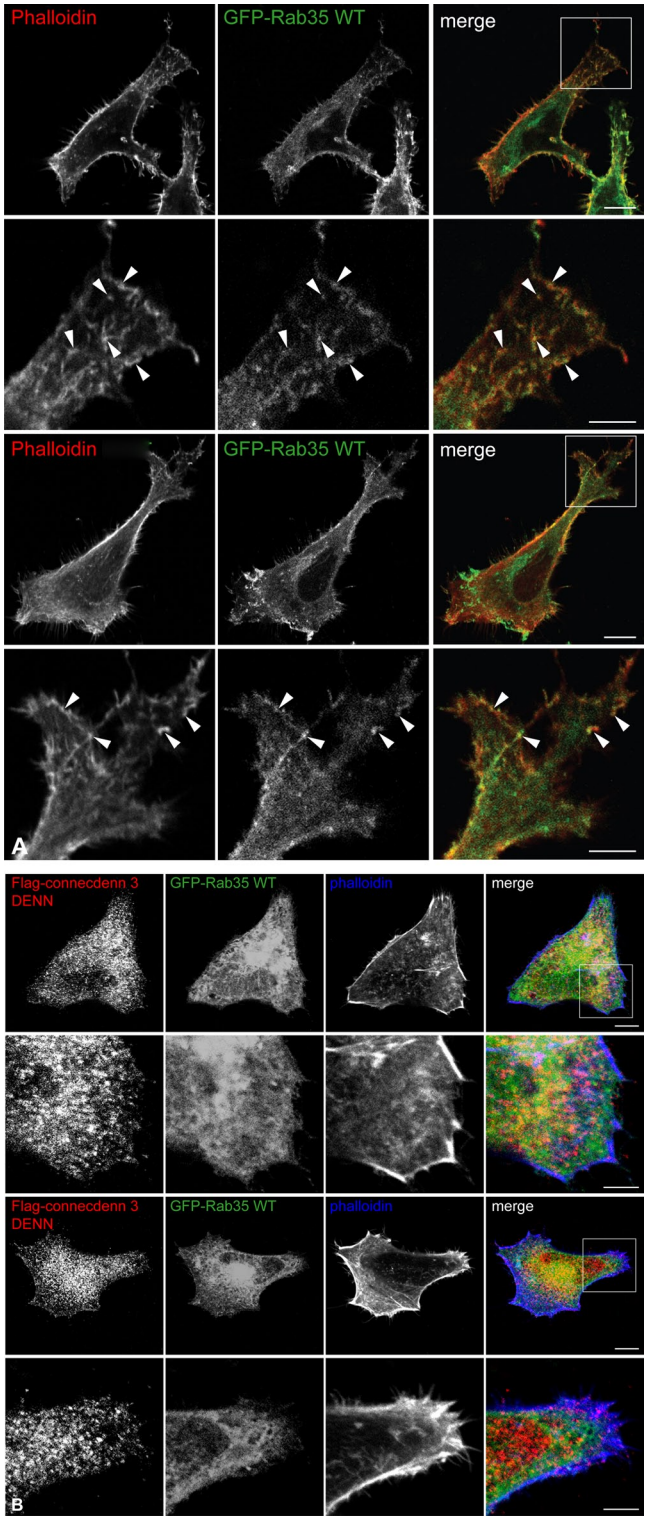

FIGURE 8: The DENN domain of connecdenn 3 has a dominant-negative effect. (A) HeLa cells were transfected with GFP-tagged wild-type (WT) Rab35 and processed for immunofluorescence. Actin was visualized by costaining with TRITC-labeled phalloidin (red). Arrowheads indicate colocalization between wild-type Rab35 and actin filaments. (B) HeLa cells were cotransfected with FLAG-tagged connecdenn 3 (CD3) DENN domain and GFP-tagged Rab35 WT and processed for immunofluorescence with a monoclonal antibody against the FLAG tag (red). Actin was visualized by costaining with Alexa Fluor 647–labeled phalloidin (blue). Scale bars, lower magnification, 10 μm; higher magnification, 5 μm.

DISCUSSION

DENN domain–containing proteins represent a new class of regulators of Rab GTPases; however, for the majority of these proteins little is known of their function outside of the Rab they target (Levivier *et al.*, 2001; Yoshimura *et al.*, 2010; Marat *et al.*, 2011). Almost all DENN-domain proteins contain other protein modules and binding motifs (Marat *et al.*, 2011). It is likely that these modules and motifs confer additional functions and properties outside of the Rab GEF activity. In addition, they may target or regulate the DENN domain, allowing for differential regulation of a Rab toward multiple functions. As an example, the Vps9 domain exhibits GEF activity toward members of the Rab5 subfamily, and different Vps9 domain–containing proteins activate Rab5 for different functions (Carney *et al.*, 2006). In this study we sought to examine why there are three GEFs that target Rab35.

Although our studies consistently demonstrate in multiple assays that connecdenn 3 is a Rab35 GEF (Figures 1 and 2; Marat and McPherson, 2010), another study indicated that connecdenn 3 is a GEF for Rab13 (Yoshimura *et al.*, 2010). Although we find that both connecdenn 2 and 3 have slight GEF activity toward Rab13, this could be promiscuous activity, as Rab35 and Rab13 belong to the same subfamily (Schwartz *et al.*, 2007). Furthermore, functional studies on the role of Rab13 are inconsistent with connecdenn 3 being its sole GEF (Yoshimura *et al.*, 2010). Rab13 is involved in trafficking between the *trans*-Golgi network and recycling endosomes (Nokes *et al.*, 2008), inconsistent with the localization of connecdenn 3 reported here. It is possible, however, that functional links do exist between connecdenn 2 or 3, Rab35, and Rab13. For example, both Rab13 and Rab35 are involved in neurite outgrowth in PC12 cells (Chevallier *et al.*, 2009; Kanno *et al.*, 2010; Sakane *et al.*, 2010), and Rab13 functions in the formation of tight junctions by mediating the endosomal recycling of occludin (Nakatsuji *et al.*, 2008). Determining possible links will require further study.

Establishing that all members of each family of DENN domain–containing proteins target a common Rab (without excluding that some members may target additional Rabs; Allaire *et al.*, 2010; Marat and McPherson, 2010; Yoshimura *et al.*, 2010; Marat *et al.*, 2011) raises the question as to why certain Rabs need multiple activators. One possible answer is that DENN domain–containing proteins exhibit tissue specific functions. For example, the DENND4A–C family of proteins exhibits GEF activity toward Rab10, which is involved in basolateral trafficking (Babbey *et al.*, 2006; Sano *et al.*, 2007; Schuck *et al.*, 2007; Shi *et al.*, 2010; Wang *et al.*, 2010; Yoshimura *et al.*, 2010). DENND4C appears to be the primary GEF required for insulin-stimulated translocation of GLUT4 in adipocytes, a process that requires active Rab10 (Sano *et al.*, 2011), suggesting that DENND4C could have a tissue-specific role in regulating GLUT4 trafficking in adipocytes. In contrast, different DENN-domain proteins could activate a common Rab toward different activities in the same cell. For example, DENND2 proteins all exhibit GEF activity toward Rab9a/b; however, all four members have a different subcellular distribution (Yoshimura *et al.*, 2010). Rab9 is involved in retrograde transport of the mannose phosphate receptor from late endosomes to the *trans*-Golgi network, as well as in the biogenesis of lysosome-related organelles (Carroll *et al.*, 2001; Kloer *et al.*, 2010). Of interest, depletion of DENND2A affected trafficking of the mannose phosphate receptor, whereas DENND2B-D had no effect on this process (Yoshimura *et al.*, 2010). Although these studies indicate that DENN–domain proteins are not necessarily redundant in their ability to activate a common Rab, they do not actually demonstrate that DENN-domain proteins from a single family target a common Rab toward different downstream effects. Our study

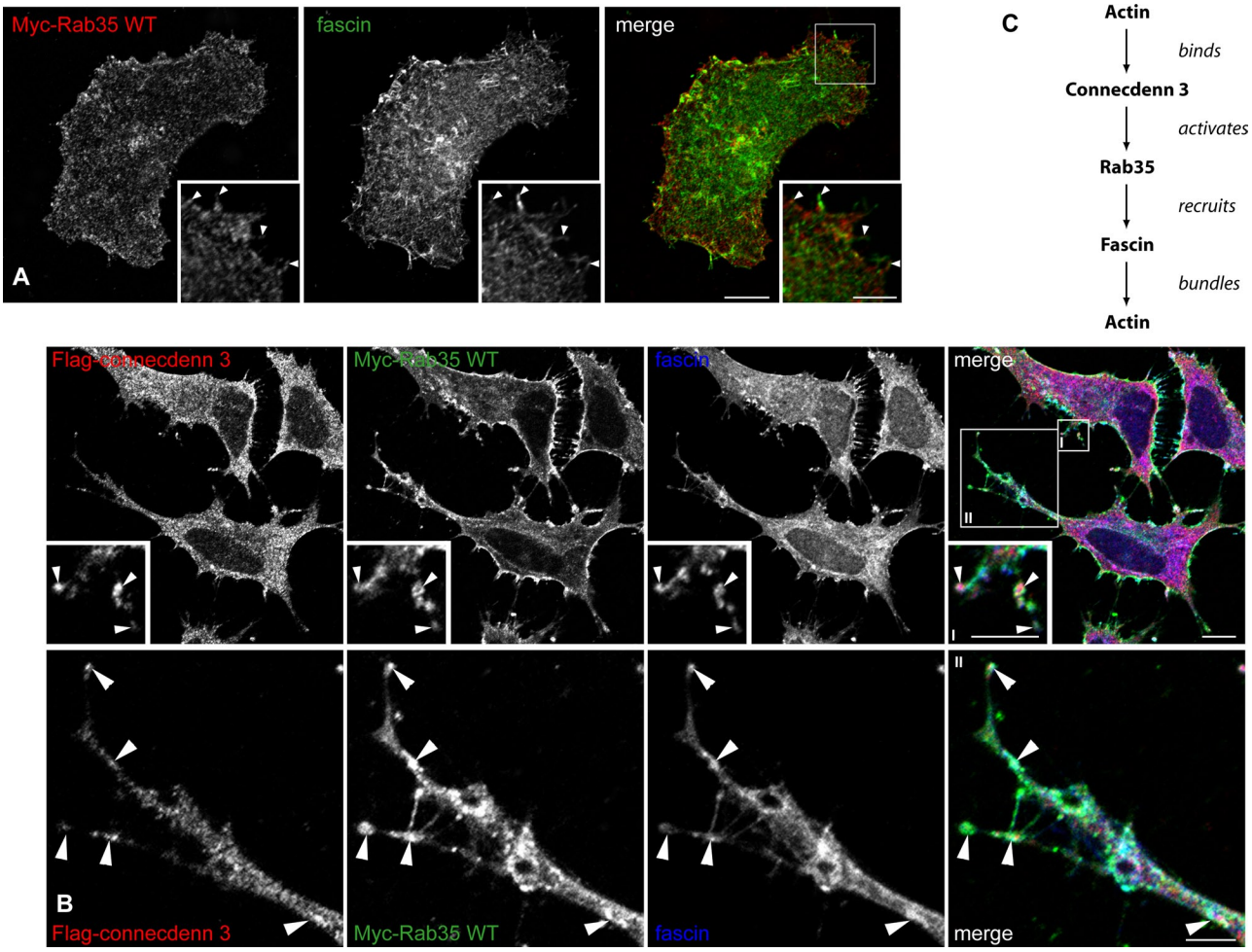

FIGURE 9: Connecdenn 3 enhances the colocalization of Rab35 and fascin. (A) HeLa cells were transfected with Myc-tagged wild-type (WT) Rab35 and processed for immunofluorescence with a polyclonal antibody against the Myc tag (red) and a monoclonal antibody against endogenous fascin (green). The area in the box is shown in the inset. Arrowheads indicate colocalization between Rab35 and fascin. Scale bars, lower magnification, 10 μm; higher magnification, 5 μm (B) HeLa cells were cotransfected with FLAG-tagged full-length connecdenn 3 and Myc-tagged wild-type (WT) Rab35 and processed for immunofluorescence with a rabbit polyclonal antibody against the FLAG-tag (red), a goat polyclonal antibody against the Myc-tag (green), and a mouse monoclonal antibody against fascin (blue). Arrowheads indicate colocalization among connecdenn 3, wild-type Rab35, and fascin. Scale bars, lower magnification, 10 μm; higher magnification I and II, 2 and 5 μm, respectively. (C) Model of the interaction between connecdenn 3, Rab35, fascin, and actin. Connecdenn 3 binds actin through its C-terminal motif, whereas through its N-terminal DENN domain it activates Rab35 at actin filaments. GTP-Rab35 then recruits its effector fascin, which bundles actin into filaments.

represents the first discerning the molecular mechanisms by which members of a DENN-domain family target their substrate Rab toward different functions via the use of binding motifs outside of the DENN domain. DENN domain–bearing proteins have diversified throughout evolution, with one in *Schizosaccharomyces pombe*, five in *Caenorhabditis elegans*, and 18 in humans (Marat *et al.*, 2011). Therefore it is quite likely that as Rabs evolved to control more diverse functions, the number of DENN domain proteins increased concomitantly to activate Rabs for these different functions.

In addition to differential regulation by the connecdenn GEFs, Rab35 also appears to be differentially regulated via tissue-specific GAPs. For example TBC1D10C/EPI64C is a Rab35 GAP expressed selectively in hematopoietic cells that, together with Rab35, regulates a recycling pathway in T cells for the formation of the immunological synapse (Patino-Lopez *et al.*, 2008). TBC1D24/Skywalker is a neuronal Rab35 GAP involved in the endosomal trafficking of synaptic vesicles (Uytterhoeven *et al.*, 2011). Consistent with an important role in synaptic transmission, TBC1D24 is mutated in familial epilepsies (Corbett *et al.*, 2010; Falace *et al.*, 2010), and in the nervous system connecdenn 1 is localized to the synapse, where it functions in the trafficking of synaptic vesicles (Allaire *et al.*, 2006). Because connecdenns 2 and 3 are both expressed ubiquitously (Marat and McPherson, 2010), this suggests that there could be both tissue- and function-specific effects of the connecdenn family members in their ability to activate Rab35, which, acting in coordination with different GAPs, provide a high degree of regulation for the activity of this important GTPase.

In addition to demonstrating that connecdenn 3 has a unique role in Rab35 activation, we described what appears to be a new actin-binding sequence, which, based on evolutionary conservation and our mutagenesis studies, has the consensus [R/K]V[A/S][D/E]LKKxFE. Although we could not find a known actin-binding motif with the

exact consensus sequence, the LKK found within this sequence, which is required for actin-binding activity, is also found in many other actin-binding proteins, such as neuron navigator 2, villin, dematin, thymosin, actobindin, UNC-53, WASP/N-WASP, spire, and verprolin (Friederich *et al.*, 1992; Vancompernolle *et al.*, 1992; Miki *et al.*, 1996; Van *et al.*, 1996; Vaduva *et al.*, 1997; Stringham *et al.*, 2002; Ducka *et al.*, 2010). Although these proteins share a common LKK within their actin-binding motif, sequences around the LKK determine the actin-binding properties of the protein. Of interest, in thymosin β4 a region N-terminal to the motif has an inhibitory effect on actin polymerization through steric hindrance (Vancompernolle *et al.*, 1992). We did not observe that the connecdenn 3 actin-binding sequence had an effect on the ratio of G- to F-actin in our sedimentation assays; therefore, it appears likely that connecdenn 3, like Rab35 (Zhang *et al.*, 2009), does not have a direct effect on actin dynamics. Instead, they control the recruitment of actin-modulating proteins.

This study provides the first example of how DENN-domain proteins have different effects on their target Rab via their localizations to different cellular compartments through binding motifs outside of the DENN domain. Because DENN domain–containing proteins represent a new class of regulators of Rab GTPases (Marat *et al.*, 2011), this highlights the importance of understanding the role of regions outside of the DENN domain.

MATERIALS AND METHODS

Antibodies and DNA constructs

Monoclonal (M2) and polyclonal FLAG antibodies were from Sigma-Aldrich (St. Louis, MO). Polyclonal rabbit and goat antibodies against the Myc-tag were from Santa Cruz Biotechnology (Santa Cruz, CA), and polyclonal tubulin antibody was from ICN Biomedical (Irvine, CA). Monoclonal antibodies against the α-adaptin subunit of AP-2, actin, and fascin (55K2) were from BD Transduction Laboratories (Lexington, KY), Chemicon (Temecula, CA), and Abcam (Cambridge, MA), respectively. Fluorescein isothiocyanate– and Alexa Fluor 647–conjugated phalloidin were from Sigma-Aldrich and Invitrogen (Carlsbad, CA), respectively.

GST-Rab1A (human amino acids [aa] 1–205 in pGEX-6P1) was cloned from GFP-Rab1A (NM_004161; a generous gift of John Presley, McGill University, Montreal, Canada), which was used as a PCR template. GST-Rab13 (human aa 1–203 in pGEX-6P1) was cloned by PCR from cDNA obtained from Open Biosystems (BC073168; Thermo Biosystems, Huntsville, AL). GST-Rab35 (human aa 1–201 in pGEX-6P1), FLAG-connecdenn 1 DENN domain (mouse aa 1–403 in pcDNA3-FLAG), FLAG- and GST-connecdenn 2 DENN domain (human aa 2–421 in pCMV-Tag2B and pEBG), FLAG- and GST-connecdenn 3 DENN domain (human aa 2–424 in pCMV-Tag2B and pEBG), FLAG-connecdenn 1 (mouse aa 1–1016 in pCMV-Tag2B), FLAG-connecdenn 2 (aa 2–775 in pcDNA3-FLAG), FLAG-connecdenn 3 (aa 2–801 in pCMV-Tag2B), myc-Rab35 wild type, S22N, and Q67L (in pcDNA3-myc), and GFP-Rab35 wild type (in peGFP-C1) were previously described (Allaire *et al.*, 2006, 2010; Marat and McPherson, 2010). FLAG-connecdenn 3 Δ786–801 and Δ1–424 (aa 2–785 and 425–801, respectively, in pCMV-Tag2B) were generated using FLAG-connecdenn 3 as a PCR template. GST-connecdenn 3 789–801 wild-type and point mutants were generated by oligo annealing and subcloned into pGEX-4T1. All constructs were verified by sequence analysis. For the sequences of the oligonucleotides used to generate the constructs, see Supplemental Table S1.

Affinity selection assays

For affinity selection assays from brain extract, frozen adult rat brain was homogenized in buffer 1 (20 mM 4-(2-hydroxyethyl)-1-piperazineethanesulfonic acid [HEPES], pH 7.4, supplemented with protease inhibitors: 0.83 mM benzamidine, 0.23 mM phenylmethylsulfonyl fluoride, 0.5 μg/ml aprotinin, and 0.5 μg/ml leupeptin) and centrifuged at 800 × *g* for 10 min, the supernatant was collected, and Triton X-100 was added to 1% final concentration. The samples were incubated for 15 min at 4°C, then centrifuged at 205,000 × *g* for 30 min. The supernatant was adjusted to a final concentration of 2 mg/ml in buffer 1 with 100 mM NaCl and 1% Triton X-100. Aliquots of 1 ml of the Triton-soluble brain extract were incubated with GST fusion proteins precoupled to glutathione–Sepharose beads. Samples were incubated for ~3 h at 4°C and washed three times with ice-cold buffer 1 containing 1% Triton X-100 and 100 mM NaCl. Samples were eluted in SDS–PAGE sample buffer, resolved by SDS–PAGE, and processed for Western blot.

For recombinant proteins, FLAG-tagged fusion proteins were expressed in HEK-293T cells. At 48 h posttransfection, cells were washed with phosphate-buffered saline (PBS; 20 mM NaH_2PO_4, 150 mM NaCl, pH 7.4), scraped into a nucleotide-free buffer (20 mM Tris, pH 7.5, protease inhibitors, 100 mM NaCl, and 5 mM EDTA) or nucleotide buffer (20 mM Tris, pH 7.5, protease inhibitors, 100 mM NaCl, 5 mM $MgCl_2$), and sonicated, and Triton X-100 was added to 1% final concentration. After 15 min of incubation at 4°C, the lysates were centrifuged at 305 000 × *g* for 20 min at 4°C. In parallel, GST-Rab fusion proteins were expressed in *Escherichia coli* BL21. After coupling to glutathione–Sepharose, GST-Rabs were exchanged into nucleotide-free buffer with 0.5 mM dithiothreitol (DTT) or GTPγS loading buffer (20 mM Tris, pH 7.5, protease inhibitors, 100 mM NaCl, and 0.5 mM DTT). GTPγS was loaded onto the GST-Rab fusion proteins by incubating with a threefold molar excess of GTPγS and 5 mM EDTA for 10 min at 30°C, followed by the addition of $MgCl_2$ to 10 mM and DTT to 0.1 mM. Aliquots of 1 ml of cell lysates in either the nucleotide-free or nucleotide condition were incubated for 1 h at 4°C with precoupled GST fusion proteins in the nucleotide-free or GTPγS-loaded state, respectively, washed three times with the corresponding ice-cold, nucleotide-free or nucleotide buffer with 1% Triton, and processed for Western blotting.

Actin monomer affinity selection assay

GST-connecdenn 3 peptides precoupled to glutathione–Sepharose were incubated for 1 h at 4°C with 1 ml of 50 mM (below the critical concentration for actin polymerization) G-actin (APHL99-A; Cytoskeleton, Denver, CO) in 100 mM KCl, 1 mM $MgCl_2$, 0.1 mM EDTA, 1 mM DTT, 0.2 mM ATP, 100 mM NaCl, and 1% Triton X-100 in buffer 1. Samples were washed two times in this buffer and eluted in SDS–PAGE sample buffer, resolved by SDS–PAGE, and processed for Western blotting.

F-actin cosedimentation assays

HeLa cells were plated in 35-mm wells in DMEM such that they would be 90% confluent 24 h postplating, at which time they were transfected with 2 μg of the different FLAG-tagged connecdenn plasmids using jetPRIME (Polyplus-transfection, Illkirch, France) according to the manufacturer's instructions. At 24 h posttransfection, cells were washed with PBS and scraped into 50 μl of lysis buffer consisting of buffer 1 with 1% NP-40. Cells were lysed on ice for 30 min, and the lysates were centrifuged at 245,000 × *g* for 1 h at 4°C. The supernatant was collected, and 10 μl was used for each condition of the cosedimentation assay. For purified protein, the indicated peptides of connecdenn 3 tagged with GST were expressed in *E. coli* BL21. Bacterial lysates were incubated with glutathione–Sepharose, and after washing, the bound proteins were

eluted with 100 mM Tris, pH 8.3, and 20 mM reduced L-glutathione. Eluted GST-connecdenn 3 peptides were then exchanged into 20 mM HEPES, pH 7.4, concentrated to 8 μg/μl, and centrifuged at 245,000 × *g* for 1 h at 4°C prior to use in the actin cosedimentation assays at the indicated molar concentrations. Actin cosedimentation assays were performed with an Actin-Binding Protein Biochem Kit: Non-Muscle Actin (BK013; Cytoskeleton), essentially as described by the manufacturer; supplied α-actinin was used as a positive control (data not shown). Briefly, protein preparations or cell lysates were incubated with 18 μM of freshly polymerized nonmuscle actin (F-actin) or F-actin buffer alone with a final concentration of 100 mM NaCl for 30 min at room temperature. Samples were centrifuged at 156,705 × *g* for 1.5 h at 22°C to pellet F-actin and cosedimenting proteins. Supernatants were collected on ice, and pellets were then resuspended on ice for 10 min in 20 mM HEPES, pH 7.4, and 100 mM NaCl in a volume equivalent to the supernatant fraction. SDS–PAGE sample buffer was added to both supernatant and pellet fractions, and the entire fractions were then resolved by SDS–PAGE and processed for Western blot or stained with Coomassie blue. Quantification of the amount of GST-connecdenn 3 peptides specifically cosedimenting with F-actin was quantified by densitometry using ImageJ (National Institutes of Health, Bethesda, MD; n = 2, mean ± SE).

Immunofluorescence

Cells grown on poly-L-lysine–coated coverslips were washed in PBS and then fixed for 20 min in 3% paraformaldehyde. After fixation, cells were permeabilized with 0.2% Triton X-100 in PBS and processed for immunofluorescence with the appropriate primary and secondary antibodies in PBS. For fascin staining, cells were fixed with ice-cold methanol at −20°C for 10 min and then processed for immunofluorescence with the appropriate primary and secondary antibodies in 1% bovine serum albumin/PBS. In other cases, cells were incubated with 1 μM latrunculin B in DMEM for 10 min at 37°C prior to fixation with 3% paraformaldehyde. For transfections, cells were plated on coverslips in DMEM such that they would be 60% confluent 24 h postplating, at which time they were transfected with 0.5 μg of the indicated plasmids, using jetPRIME according to the manufacturer's instructions. Cells were processed for immunofluorescence at 18 h posttransfection. Images were obtained using a Zeiss (Thornwood, NY) 700 or 710 Laser Scanning Confocal Microscope. Quantification of colocalization between FLAG-connecdenn 3 and phalloidin labeled F-actin was done by taking 111 Z-stack images from 11 cells at an interval of 0.36 μm. Percentage colocalization was determined by analyzing the degree of particle overlap using ImageJ.

In vitro GDP/GTP exchange assays

GST-tagged Rab13 and Rab35 were expressed in *E. coli* BL21. Bacteria were resuspended in PBS with protease inhibitors and sonicated, and Triton X-100 was added to 1% final concentration. The lysates were incubated for 30 min at 4°C and spun at 30,700 × *g* for 10 min. The supernatant was incubated with glutathione–Sepharose beads for 3 h at 4°C and washed three times in PreScission protease cleavage buffer (GE Healthcare, Piscataway, NJ; 20 mM Tris, pH 7.0, 150 mM NaCl, 1 mM dithiothreitol, 1 mM EDTA), and the purified fusion proteins were cleaved from the GST tag by overnight incubation with PreScission protease at 4°C. Cleaved GTPases were then exchanged into GEF loading buffer (20 mM Tris, pH 7.5, 100 mM NaCl). Purified connecdenn 2 and 3 DENN domains were made from GST-tagged proteins expressed in HEK-293T cells as previously described (Marat and McPherson, 2010). FLAG-tagged connecdenn 3 full length was expressed in HEK-293T cells. At 48 h posttransfection, cells were collected in PBS with protease inhibitors and sonicated, and Triton X-100 was added to 1% final concentration. The lysates were incubated for 30 min at 4°C and spun at 21,000 × *g* for 15 min. The supernatant was incubated with 12.5 μl of Protein G-Sepharose (GE Healthcare) and 5 μg of monoclonal FLAG (M2) antibody for 3 h at 4°C and washed in GEF incubation buffer (20 mM Tris, pH 7.5, 100 mM NaCl, and 5 mM $MgCl_2$). Immunoprecipitated protein coupled to Protein G-Sepharose was then immediately added to the in vitro GDP/GTP exchange assays, while a duplicate immunoprecipitation was eluted in SDS–PAGE sample buffer, resolved by SDS–PAGE, and processed for Western blotting. GEF assays were performed essentially as previously described (Marat and McPherson, 2010). Briefly, 15 μM of purified Rab GTPases were loaded with 30 μM GDP (Sigma-Aldrich) by incubation for 10 min at 30°C in GEF loading buffer (20 mM Tris, pH 7.5, 100 mM NaCl) with 5 mM EDTA; loaded GDP was then stabilized by the addition of 10 mM $MgCl_2$. Exchange reactions were carried out at room temperature in 65 μl of total volume containing 1.25 μM loaded GTPase, 350 nM purified DENN domain, or immunoprecipated FLAG-connecdenn 3, 0.5 mg/ml bovine serum albumin, 5 μM GTPγS (Sigma-Aldrich), 0.2 mCi/mmol [^{35}S]GTPγS (PerkinElmer, Waltham, MA), and 0.5 mM DTT in GEF incubation buffer (20 mM Tris, pH 7.5, 100 mM NaCl, and 5 mM $MgCl_2$). At the indicated times, 15 μl of the reaction was removed, added to 1 ml ice-cold wash buffer (20 mM Tris, pH 7.5, 100 mM NaCl, 20 mM $MgCl_2$), and passed through nitrocellulose filters. The filters were rapidly washed with 5 ml of wash buffer and counted using a liquid scintillation counter (LS6500 Scintillator; Beckmann Coulter, Brea, CA). Data were plotted in GraphPad Prism 4 (GraphPad Software, La Jolla, CA) and curve fitted by a nonlinear regression one-phase association. Experiments were performed with purified DENN domain (n = 2, mean ± SE); for immunoprecipitated protein a representative experiment is shown.

ACKNOWLEDGMENTS

We thank John Presley for the generous gift of constructs, as well as Jacynthe Philie and Martine Girard for excellent technical assistance. This work was supported by Grant MOP-15396 from the Canadian Institutes of Health Research to P.S.M. M.S.I is supported by a Frederick Banting and Charles Best Canada Graduate Scholarship from the Canadian Institutes of Health Research. A.L.M was supported by a Fonds de la Recherche en Santé du Québec fellowship and a McGill University Faculty of Medicine Lloyd Carr-Harris Fellowship. P.S.M. is a James McGill Professor.

REFERENCES

Adams JC, Clelland JD, Collett GD, Matsumura F, Yamashiro S, Zhang L (1999). Cell-matrix adhesions differentially regulate fascin phosphorylation. Mol Biol Cell 10, 4177–4190.

Allaire PD, Marat AL, Dall'Armi C, Di PG, McPherson PS, Ritter B (2010). The Connecdenn DENN domain: a GEF for Rab35 mediating cargo-specific exit from early endosomes. Mol Cell 37, 370–382.

Allaire PD, Ritter B, Thomas S, Burman JL, Denisov AY, Legendre-Guillemin V, Harper SQ, Davidson BL, Gehring K, McPherson PS (2006). Connecdenn, a novel DENN domain-containing protein of neuronal clathrin-coated vesicles functioning in synaptic vesicle endocytosis. J Neurosci 26, 13202–13212.

Babbey CM, Ahktar N, Wang E, Chen CC, Grant BD, Dunn KW (2006). Rab10 regulates membrane transport through early endosomes of polarized Madin-Darby canine kidney cells. Mol Biol Cell 17, 3156–3175.

Carney DS, Davies BA, Horazdovsky BF (2006). Vps9 domain-containing proteins: activators of Rab5 GTPases from yeast to neurons. Trends Cell Biol 16, 27–35.

Carroll KS, Hanna J, Simon I, Krise J, Barbero P, Pfeffer SR (2001). Role of Rab9 GTPase in facilitating receptor recruitment by TIP47. Science 292, 1373–1376.
Chevallier J, Koop C, Srivastava A, Petrie RJ, Lamarche-Vane N, Presley JF (2009). Rab35 regulates neurite outgrowth and cell shape. FEBS Lett 583, 1096–1101.
Chua CE, Lim YS, Tang BL (2010). Rab35—a vesicular traffic-regulating small GTPase with actin modulating roles. FEBS Lett 584, 1–6.
Corbett MA *et al.* (2010). A focal epilepsy and intellectual disability syndrome is due to a mutation in TBC1D24. Am J Hum Genet 87, 371–375.
Delprato A, Merithew E, Lambright DG (2004). Structure, exchange determinants, and family-wide Rab specificity of the tandem helical bundle and Vps9 domains of Rabex-5. Cell 118, 607–617.
dos Remedios CG, Chhabra D, Kekic M, Dedova IV, Tsubakihara M, Berry DA, Nosworthy NJ (2003). Actin binding proteins: regulation of cytoskeletal microfilaments. Physiol Rev 83, 433–473.
Ducka AM, Joel P, Popowicz GM, Trybus KM, Schleicher M, Noegel AA, Huber R, Holak TA, Sitar T (2010). Structures of actin-bound Wiskott-Aldrich syndrome protein homology 2 (WH2) domains of Spire and the implication for filament nucleation. Proc Natl Acad Sci USA 107, 11757–11762.
Falace A *et al.* (2010). TBC1D24, an ARF6-interacting protein, is mutated in familial infantile myoclonic epilepsy. Am J Hum Genet 87, 365–370.
Friederich E, Vancompernolle K, Huet C, Goethals M, Finidori J, Vandekerckhove J, Louvard D (1992). An actin-binding site containing a conserved motif of charged amino acid residues is essential for the morphogenic effect of villin. Cell 70, 81–92.
Fukuda M (2011). TBC proteins: GAPs for mammalian small GTPase Rab? Biosci Rep 31, 159–168.
Gao Y, Balut CM, Bailey MA, Patino-Lopez G, Shaw S, Devor DC (2010). Recycling of the Ca2+-activated K+ channel, KCa2.3, is dependent upon RME-1, Rab35/EPI64C, and an N-terminal domain. J Biol Chem 285, 17938–17953.
Heo WD, Inoue T, Park WS, Kim ML, Park BO, Wandless TJ, Meyer T (2006). PI(3,4,5)P3 and PI(4,5)P2 lipids target proteins with polybasic clusters to the plasma membrane. Science 314, 1458–1461.
Heo WD, Meyer T (2003). Switch-of-function mutants based on morphology classification of Ras superfamily small GTPases. Cell 113, 315–328.
Hsu C *et al.* (2010). Regulation of exosome secretion by Rab35 and its GTPase-activating proteins TBC1D10A-C. J Cell Biol 189, 223–232.
Hussain NK *et al.* (2001). Endocytic protein intersectin-l regulates actin assembly via Cdc42 and N-WASP. Nat Cell Biol 3, 927–932.
Hutagalung AH, Novick PJ (2011). Role of Rab GTPases in membrane traffic and cell physiology. Physiol Rev 91, 119–149.
Kanno E, Ishibashi K, Kobayashi H, Matsui T, Ohbayashi N, Fukuda M (2010). Comprehensive screening for novel Rab-binding proteins by GST pull-down assay using 60 different mammalian Rabs. Traffic 11, 491–507.
Kloer DP, Rojas R, Ivan V, Moriyama K, Ivan V, Murthy N, Ghirlando R, van der Sluijs P, Hurley JH, Bonifacino JS (2010). Assembly of the biogenesis of lysosome-related organelles complex-3 (BLOC-3) and its interaction with Rab9. J Biol Chem 285, 7794–7804.
Kouranti I, Sachse M, Arouche N, Goud B, Echard A (2006). Rab35 regulates an endocytic recycling pathway essential for the terminal steps of cytokinesis. Curr Biol 16, 1719–1725.
Levivier E, Goud B, Souchet M, Calmels TP, Mornon JP, Callebaut I (2001). uDENN, DENN, and dDENN: indissociable domains in Rab and MAP kinases signaling pathways. Biochem Biophys Res Commun 287, 688–695.
Liao Y *et al.* (1999). RA-GEF, a novel Rap1A guanine nucleotide exchange factor containing a Ras/Rap1A-associating domain, is conserved between nematode and humans. J Biol Chem 274, 37815–37820.
Liao Y, Satoh T, Gao X, Jin TG, Hu CD, Kataoka T (2001). RA-GEF-1, a guanine nucleotide exchange factor for Rap1, is activated by translocation induced by association with Rap1*GTP and enhances Rap1-dependent B-Raf activation. J Biol Chem 276, 28478–28483.
Marat AL, Dokainish H, McPherson PS (2011). DENN domain proteins: regulators of Rab GTPases. J Biol Chem 286, 13791–13800.
Marat AL, McPherson PS (2010). The connecdenn family, Rab35 guanine nucleotide exchange factors interfacing with the clathrin machinery. J Biol Chem 285, 10627–10637.
Miki H, Miura K, Takenawa T (1996). N-WASP, a novel actin-depolymerizing protein, regulates the cortical cytoskeletal rearrangement in a PIP2-dependent manner downstream of tyrosine kinases. EMBO J 15, 5326–5335.
Nakatsuji H, Nishimura N, Yamamura R, Kanayama HO, Sasaki T (2008). Involvement of actinin-4 in the recruitment of JRAB/MICAL-L2 to cell-cell junctions and the formation of functional tight junctions. Mol Cell Biol 28, 3324–3335.
Nokes RL, Fields IC, Collins RN, Folsch H (2008). Rab13 regulates membrane trafficking between TGN and recycling endosomes in polarized epithelial cells. J Cell Biol 182, 845–853.
Patino-Lopez G, Dong X, Ben-Aissa K, Bernot KM, Itoh T, Fukuda M, Kruhlak MJ, Samelson LE, Shaw S (2008). Rab35 and its GAP EPI64C in T cells regulate receptor recycling and immunological synapse formation. J Biol Chem 283, 18323–18330.
Saito K, Murai J, Kajiho H, Kontani K, Kurosu H, Katada T (2002). A novel binding protein composed of homophilic tetramer exhibits unique properties for the small GTPase Rab5. J Biol Chem 277, 3412–3418.
Sakane A, Honda K, Sasaki T (2010). Rab13 regulates neurite outgrowth in PC12 cells through its effector protein, JRAB/MICAL-L2. Mol Cell Biol 30, 1077–1087.
Sano H, Eguez L, Teruel MN, Fukuda M, Chuang TD, Chavez JA, Lienhard GE, McGraw TE (2007). Rab10, a target of the AS160 Rab GAP, is required for insulin-stimulated translocation of GLUT4 to the adipocyte plasma membrane. Cell Metab 5, 293–303.
Sano H, Peck GR, Kettenbach AN, Gerber SA, Lienhard GE (2011). Insulin-stimulated GLUT4 protein translocation in adipocytes requires the Rab10 guanine nucleotide exchange factor Dennd4C. J Biol Chem 286, 16541–16545.
Sato M, Sato K, Liou W, Pant S, Harada A, Grant BD (2008). Regulation of endocytic recycling by *C. elegans* Rab35 and its regulator RME-4, a coated-pit protein. EMBO J 27, 1183–1196.
Schoebel S, Oesterlin LK, Blankenfeldt W, Goody RS, Itzen A (2009). RabGDI displacement by DrrA from *Legionella* is a consequence of its guanine nucleotide exchange activity. Mol Cell 36, 1060–1072.
Schuck S, Gerl MJ, Ang A, Manninen A, Keller P, Mellman I, Simons K (2007). Rab10 is involved in basolateral transport in polarized Madin-Darby canine kidney cells. Traffic 8, 47–60.
Schwartz SL, Cao C, Pylypenko O, Rak A, Wandinger-Ness A (2007). Rab GTPases at a glance. J Cell Sci 120, 3905–3910.
Shi A, Chen CC, Banerjee R, Glodowski D, Audhya A, Rongo C, Grant BD (2010). EHBP-1 functions with RAB-10 during endocytic recycling in *Caenorhabditis elegans*. Mol Biol Cell 21, 2930–2943.
Shim J, Lee SM, Lee MS, Yoon J, Kweon HS, Kim YJ (2010). Rab35 mediates transport of Cdc42 and Rac1 to the plasma membrane during phagocytosis. Mol Cell Biol 30, 1421–1433.
Stenmark H (2009). Rab GTPases as coordinators of vesicle traffic. Nat Rev Mol Cell Biol 10, 513–525.
Stringham E, Pujol N, Vandekerckhove J, Bogaert T (2002). unc-53 controls longitudinal migration in *C. elegans*. Development 129, 3367–3379.
Uytterhoeven V, Kuenen S, Kasprowicz J, Miskiewicz K, Verstreken P (2011). Loss of skywalker reveals synaptic endosomes as sorting stations for synaptic vesicle proteins. Cell 145, 117–132.
Vaduva G, Martin NC, Hopper AK (1997). Actin-binding verprolin is a polarity development protein required for the morphogenesis and function of the yeast actin cytoskeleton. J Cell Biol 139, 1821–1833.
Van TM, Dewitte D, Goethals M, Carlier MF, Vandekerckhove J, Ampe C (1996). The actin binding site of thymosin beta 4 mapped by mutational analysis. EMBO J 15, 201–210.
Vancompernolle K, Goethals M, Huet C, Louvard D, Vandekerckhove J (1992). G- to F-actin modulation by a single amino acid substitution in the actin binding site of actobindin and thymosin beta 4. EMBO J 11, 4739–4746.
Vignjevic D, Kojima S, Aratyn Y, Danciu O, Svitkina T, Borisy GG (2006). Role of fascin in filopodial protrusion. J. Cell Biol 174, 863–875.
Walseng E, Bakke O, Roche PA (2008). Major histocompatibility complex class II-peptide complexes internalize using a clathrin- and dynamin-independent endocytosis pathway. J Biol Chem 283, 14717–14727.
Wang D, Lou J, Ouyang C, Chen W, Liu Y, Liu X, Cao X, Wang J, Lu L (2010). Ras-related protein Rab10 facilitates TLR4 signaling by promoting replenishment of TLR4 onto the plasma membrane. Proc Natl Acad Sci USA 107, 13806–13811.
Yoshimura S, Gerondopoulos A, Linford A, Rigden DJ, Barr FA (2010). Family-wide characterization of the DENN domain Rab GDP-GTP exchange factors. J Cell Biol 191, 367–381.
Zerial M, McBride H (2001). Rab proteins as membrane organizers. Nat Rev Mol Cell Biol 2, 107–117.
Zhang J, Fonovic M, Suyama K, Bogyo M, Scott MP (2009). Rab35 controls actin bundling by recruiting fascin as an effector protein. Science 325, 1250–1254.